A COMPARISON OF LOCAL PHOSPHORESCENCE DETECTION AND FLUID DYNAMIC GAUGING METHODS FOR STUDYING THE REMOVAL OF COHESIVE FOULING LAYERS: EFFECT of layer

Patrick W. Gordon[a], Martin Schöler[b], Henning Föste[c], Manuel Helbig[b], Wolfgang Augustin[c], Y.M. John Chew[d], Stephan Scholl[c], Jens-Peter Majschak[b], D. Ian Wilson[a]*.

[a] Department of Chemical Engineering and Biotechnology, University of Cambridge, New Museums Site, Pembroke Street, Cambridge, CB2 3RA, UK.

[b] Institute of Processing Machines and Mobile Machines, Faculty of Mechanical Engineering, Technische Universität Dresden, Dresden, Germany.

[c] Institute for Chemical and Thermal Process Engineering, Technische Universität Braunschweig, Braunschweig, Germany.

[d] Department of Chemical Engineering, University of Bath, Claverton Down, Bath, BA2 7AY, UK.

* Corresponding author. Email: diw11@cam.ac.uk; Tel: +44 (0)1223 (3)34791

revised manuscript

July 2013

1

A COMPARISON OF LOCAL PHOSPHORESCENCE DETECTION AND FLUID DYNAMIC GAUGING METHODS FOR STUDYING THE REMOVAL OF COHESIVE FOULING LAYERS: EFFECT OF LAYER ROUGHNESS

Patrick W. Gordon[a], Martin Schöler[b], Henning Föste[c], Manuel Helbig[b], Wolfgang Augustin[c], Y.M. John Chew[d], Stephan Scholl[c], Jens-Peter Majschak[b], D. Ian Wilson[a]*.

[a] Department of Chemical Engineering and Biotechnology, University of Cambridge, New Museums Site, Pembroke Street, Cambridge, CB2 3RA, UK.

[b] Institute of Processing Machines and Mobile Machines, Faculty of Mechanical Engineering, Technische Universität Dresden, Dresden, Germany.

[c] Institute for Chemical and Thermal Process Engineering, Technische Universität Braunschweig, Braunschweig, Germany.

[d] Department of Chemical Engineering, University of Bath, Claverton Down, Bath, BA2 7AY, UK.

* Corresponding author. Email: diw11@cam.ac.uk; Tel: +44 (0)1223 (3)34791

ABSTRACT

The performance of industrial cleaning in place (CIP) procedures is critically important for food manufacture. CIP has yet to be optimised for many processes, in part since the mechanisms involved in cleaning are not fully understood. Laboratory tests have an important role in guiding industrial trials, and this paper introduces and compares two experimental techniques developed for studying CIP mechanisms: local phosphorescence detection (LPD), and scanning fluid dynamic gauging (sFDG).

To illustrate the comparison, each technique is used to investigate the influence of soil topology on the cleaning of pre-gelatinised starch-based layers from 316 stainless steel substrates by aqueous NaOH solutions at ambient temperature. The roughness of the soil

surface is varied by incorporating zinc sulphide particles with different particle size distributions (range 1 - 80 μm) into the starch suspensions. The soil roughness increased with the use of larger particles, increasing the 3D arithmetic mean roughness (S_a) of the dry layers (range 0.37 - 3.33 μm). Rough layers were cleaned more readily than those containing small inclusions, with a good correlation between the cleaning rates observed during LPD and FDG measurements. The LPD technique, which is an instrumented CIP test, gives a better indication of the cleaning time, while sFDG measurements provide further insight into the removal mechanisms.

Keywords: Cleaning, Starch, Roughness, Local Phosphorescence Detection (LPD), Fluid Dynamic Gauging (FDG).

NOMENCLATURE

Roman

D_h	[m]	Hydraulic diameter
d_n	[mm]	Nozzle inner diameter
f	[-]	Darcy friction factor
h	[mm]	Nozzle-layer separation
h_o	[mm]	Nozzle-substrate separation
I^*	[-]	Normalised phosphorescent intensity
I_s	[arb.]	Phosphorescent intensity
I_{so}	[arb.]	Initial phosphorescent intensity
m_f	[g s^{-1}]	Mass flow rate
m_s	[g]	Mass of soil
m_{so}	[g]	Initial mass of soil
p_o	[Pa]	Ambient pressure in FDG tank
p_1	[Pa]	Pressure downstream of FDG nozzle
Δp_H	[Pa]	Hydrostatic pressure difference
r_c	[-]	Weibull process characteristic rate
Re	[-]	Reynolds number
R_{FDG}	[μm s^{-1}]	FDG removal rate
R_{LPD}	[μm s^{-1}]	LPD removal rate
S_a	[μm]	3D arithmetic mean roughness
S_{pk}	[μm]	3D peak roughness
t	[s]	Time
t_c	[s]	Weibull process characteristic time
v	[m s^{-1}]	Liquid velocity

Greek

δ	[μm]	Layer thickness
ρ	[kg m^{-3}]	Liquid density
τ_w	[Pa]	Shear stress on the wall

4

Superscripts and subscripts

max   Maximum

mean   Arithmetic mean

Abbreviations

CIP   Cleaning in place

CFD   Computational fluid dynamics

FDG   Fluid dynamic gauging

LPD   Local phosphorescence detection

NaOH   Sodium hydroxide

PMMA   Poly(methyl methacrylate)

PVC   Poly(vinyl chloride)

RO   Reverse osmosis

sFDG   Scanning fluid dynamic gauge

1. INTRODUCTION

Cleaning-in-place (CIP) operations are widespread in the food sector. Ensuring the effectiveness of these procedures is essential for hygienic operation and sustainable food manufacturing. CIP operations require appreciable capital investment and resources including chemicals and energy, with concomitant impacts on waste and carbon footprint. There is therefore an on-going need to optimise these processes, both by industrial testing and through research into the mechanisms involved in cleaning.

Fryer and Asteriadou (2009) introduced a prototype cleaning map as a tool to aid qualitative categorisation and comparison of cleaning scenarios likely to arise in the food industry and related sectors. They characterised CIP actions according to the nature of the soil and of the cleaning solution. The cohesive soils studied in this work, requiring chemical agents to swell and soften the material before removal, fit into their Type 3 cleaning scenario. While the cleaning map approach provides a simple means of categorising cleaning scenarios, other factors will also influence the ease of cleaning. Amongst these, the topography of the soil

layer, and in particular its roughness (Albert *et al*., 2011), has received little attention. Whilst industry cannot generally influence the topography of the soil deposit, the roughness of this fouling layer may influence its interaction with the cleaning solution, the forces exerted by the fluid, and consequently the effectiveness of CIP operations.

This paper reports a short study of the effect of soil roughness on removal during contact with alkaline solutions at ambient temperature, and compares the information provided by two different testing techniques. Cleaning is an interdisciplinary topic (Wilson, 2005) and combines aspects of materials science, fluid flow, surface science and rheology. The need to study and optimise cleaning processes has led to the development of a number of specialised research techniques, including flow cells (Bakker *et al*., 2003; Detry *et al*., 2007), packed beds (Jurado *et al*., 2007), ultrasonic techniques (Lohr and Rose, 2003), laser sensors (Mendret *et al*., 2007), micromanipulation devices (Liu *et al*., 2006), local phosphorescence detection (LPD; Schöler *et al*., 2009) and fluid dynamic gauging (sFDG; Gordon *et al*., 2010).

The objectives of this work are to:

i. Discuss, compare and contrast the LPD and sFDG techniques within the context of industrial CIP research.

ii. Illustrate this comparison by conducting a brief study into the cleaning of starch-based layers from stainless steel substrates. This study will investigate the influence of soil topography on cleaning, using both the LPD and sFDG techniques.

The LPD technique measures the amount of soil on a surface by periodic illumination of a phosphorescent tracer (Schöler *et al*., 2009). In the experiments reported here, LPD is used to map the distribution and quantify the cleaning of starch-based deposits in a pilot-scale CIP apparatus in situ and in real time. The soil is modified by the inclusion of tracer particles, which are also used to impart surface roughness. The FDG technique measures the thickness of soft soil layers immersed in liquid by sucking liquid into a nozzle placed close to, but not touching the soil (Gordon *et al*., 2010). The sFDG technique employs a mobile gauging nozzle that can make local measurements of soil thickness and strength at several locations. Soil 'strength' here is a measure of how the soil responds to a shear stress imposed on it by

the cleaning liquid: this is calculated from analytical analysis, supported by computational fluid dynamics (CFD) simulations (Chew *et al*., 2004). FDG does not require modification of the deposit, but thickness measurements do require the deposit to retain its shape during the 5 - 10 s test duration.

Figure 1 shows a cross-section through a pipe wall during CIP, reproduced from Schöler *et al*. (2012). In general, either transport to (process #1), reaction within (#2) or transport from (#3) the soil can control the rate of removal during CIP. Which of these processes controls removal depends strongly on the nature of the soil and substrate, as well as on the chemical, thermal and mechanical conditions. Schöler *et al*. (2012) showed that, for similar starch-based layers to those employed in the current work, process #3 controls the rate of material removal.

2. MATERIALS AND METHODS

2.1. Model Food Soil

The model food soil used in this work consisted of an instant, pre-gelatinised and homogenised waxy maize starch (C-Tex 12616, Cargill) mixed with a particulate tracer and dried into a thin layer. Zinc sulphide (ZnS) crystals were chosen as a material suitable for use both as the phosphorescent tracer necessary for LPD measurements, and as an artificial cause of soil roughness. ZnS powder was sourced from two suppliers (Lumilux Green, Honeywell, USA; Storelite, RC Tritec AG, Switzerland), while further particle size variations (Table 1) were achieved by dry sieving using different mesh sizes.

Model food soil samples were prepared by mixing 17 g starch with 23 g of phosphorescent particles, and stirring into 230 g of reverse osmosis (RO) water at 1000 rpm for 30 min. The paste was applied to the substrate (316 stainless steel, 0.14 μm 2D arithmetic mean

roughness) using a temporary polyvinyl chloride mask (PVC, 60 μm thick), giving a thin film that dried at room temperature to form a soil layer 5 - 10 μm thick. The volume fraction of ZnS particles in the wet layer was estimated as ~ 2 vol% and approximately 30 vol% when dry. For LPD testing, the starch-based layer was formed directly onto the inner wall of the cylindrical test section (26 mm inner diameter) using a 13×210 mm mask (

Figure 2). For ease of transport and measurement, sFDG samples were prepared on small metal coupons of similar surface finish, using a 5×20 mm mask.

2.2.   LPD Cleaning Tests

A detailed description of the LPD test rig (

Figure 2) is given in Schöler *et al*. (2009, 2012). Aqueous cleaning solution is circulated from holding tanks, through the test section, at a specified flow rate. The test region consists of a straight cylindrical pipe section (26 mm internal diameter, 150 mm length, 1.5 m entry/exit lengths) and comprises two parts: a 316 stainless steel lower surface, onto which the soil is applied; and a detachable transparent polymethyl methacrylate (PMMA) upper surface, allowing illumination and detection. The system closely replicates the geometry and behaviour of an industrial CIP system, allowing experimental results to be extrapolated to an industrial scale with confidence.

Measurement of the LPD cleaning progress is conducted *in situ*, by repeated illumination and detection of the local soil phosphorescence. A custom-built LED light source is used to illuminate the test region for 10 s, followed by a 1 s delay, CCD image capture (Nikon D200 camera), and a further 1 s delay. This cycle is repeated throughout the CIP test to achieve locally and temporally resolved measurement of the cleaning progress. An opaque housing around the test region ensures that only ZnS phosphorescence is detected.

LPD tests were conducted in Dresden, at room temperature, with a static gauge pressure within the test region of 150 mbar. The system, including sample, was first rinsed with tap water for 2 min (causing the layer to rehydrate to its original wet thickness, as confirmed by separate sFDG measurements) before contact with the cleaning solution (0.5 wt% NaOH) for 30 min. The flow rate of both liquids was controlled to give a consistent mean velocity of 1.0 m s^{-1} within the test region.

Image processing is conducted by cropping within ImageJ™ software, calculating the brightness and regression using Matlab™, and plotting using Origin™. The cleaning progress is characterised by assuming a fit to a two-parameter Weibull distribution, proposed for quantifying cleaning by Dürr (2002):

$$1 - \frac{I_s}{I_{so}} = 1 - I* \qquad (1)$$

$$= 1 - \exp\left(-\left(\frac{t}{t_c}\right)^{r_c}\right) = 1 - \frac{m_s}{m_{so}}$$

where I_s is the phosphorescent intensity at time t, I_{so} is the initial phosphorescent intensity, I^* is the normalised phosphorescent intensity, t is the elapsed cleaning time, the Weibull parameters t_c and r_c characterise the cleaning process, m_s is the mass of soil remaining and m_{so} is the original mass. The phosphorescent intensity has previously been shown to be proportional to the mass of soil previously (Schöler, 2011).

2.3. sFDG Cleaning Tests

Fluid dynamic gauging (FDG) exploits liquid flow dynamics to measure the position of a surface; its use in cleaning studies stems from the fact that the flowing liquid can be a cleaning solution, and the measured surface can be a soft layer undergoing cleaning. Details of the scanning FDG technique and computer controlled device used in this work are given in Gordon *et al.* (2010). A small nozzle (1 mm throat diameter, d_n) is positioned close to the layer, as shown in

Figure 3, and the surrounding cleaning liquid is drawn into it by a fixed suction force (Δp_H). The flow rate into the nozzle, m_f, is typically low and laminar, and is sensitive to the separation between the nozzle and the layer, h, when $h/d_n < 0.25$. The thickness of the layer, δ, is obtained by difference ($\delta = h_o - h$), where h_o is the location of the nozzle relative to the substrate. During cleaning tests, the shear stress induced by the FDG gauging flow can aid cleaning of the layer relative to that observed in a static system. Analytical approximations, validated using computational fluid dynamics (CFD) studies (Chew *et al.*, 2004), are used to estimate the shear stress imposed on the layer and thus exploit this effect.

Cleaning tests (0.5 wt% NaOH, 23 °C) using this device were conducted in Cambridge, with a feedback control loop positioning the sFDG nozzle 220 ± 20 μm above the layer surface, in order to maintain a consistent shear stress (13 ± 5 Pa) on the layer during measurement. The thickness of each sample was measured at three locations spaced 5 mm apart, in order to assess any intra-sample variation. One location was measured half as often as the others, in order to track the influence of the gauging flow on cleaning performance. The position of the substrate was determined after each experiment by measurement above a clean substrate.

3. RESULTS AND DISCUSSION

3.1. Model Food Soil Characterisation

Table 1 shows a summary of the different sample types, alongside measures of the roughness of the resulting dry model food layer (Calvimontes, 2009), as measured optically by a chromatic white light sensor (MicroGlider, Fries Research & Technology GmbH, Germany). The table demonstrates that a range of soil surface morphologies could be obtained by dry sieving the ZnS. The images of relatively rough and smooth layers in Figure 4 demonstrate the substantial differences in layer topology and that the ZnS particles were distributed evenly throughout the layer.

3.2. Influence of Food Soil Topography

The ease of cleaning each model food soil in Table 1 was quantified using the LPD system, with three replicates for each test.

Figure 5 shows typical cleaning curves for layers containing small (L2) and large (L5) tracer particles, with a Weibull fit to the data according to Equation (1). This cleaning model fitted most data sets well, with the parameters obtained reported in Table 1. The phosphorescent intensity decreases smoothly as the layer is removed, with no detectable material remaining by the end of all tests (30 min). The intensity decreases more rapidly for the layer containing larger particles, implying that the particle size influences the cleaning kinetics and/or the cleaning mechanism.

The removal behaviour for all layers can be divided into three regions, as indicated for sample L2 on the figure:

i.   An initial period during which the phosphorescent intensity decreases.

ii.   A region of rapid removal, during which the bulk of the layer is removed.

iii.   A final slow decay in the intensity.

sFDG testing allowed the swelling and removal characteristics of the starch-tracer layers to be investigated in further detail, with two replicates for each test. Thickness measurements on the pure starch layer (without ZnS additive,

Figure 6(a), measured at three different points on the layer surface) showed rapid rehydration in reverse osmosis water (pH 6.5) to the original wet film thickness (~ 60 μm) in less than 1 min, and little swelling or removal thereafter. This result justifies the LPD testing protocol, although direct comparison with LPD is not possible without ZnS tracer. In contrast,

Figure 6(b) shows that contact with 0.5 wt% NaOH solution (pH 13.1) causes rapid rehydration and swelling to over three times the original wet thickness, and is followed by a decay in thickness as the soft layer is removed.

Figure 6(c) shows the thickness of a layer (L2) shortly after immersion in 0.5 wt% NaOH solution. Rehydration and swelling of the layer is very rapid, reaching a thickness of 170 - 200 μm. The extent of swelling at this point is three times the thickness of the original layer (before drying), contributing to a weakening of the material, and subsequent flow-induced removal. Good agreement of swelling and removal behaviour was observed both for different points within a sample, and during repeated experiments. The third point on each layer was gauged half as often as the other two; hence this point required significantly longer to be cleaned, in spite of exhibiting a similar rate of removal during the act of measurement itself. Little removal was observed on parts of the layer that had not been exposed to the gauging flow, indicating that the removal mechanism involved shear-assisted material breakdown or advective mass transfer.

The profiles for other layers showed similar initial extents of swelling, but the subsequent removal rate showed a dependence on the size fraction of tracer used to prepare the layer. Samples prepared with large particles (

Figure 6(d), L5) tended to be removed more rapidly than those prepared using smaller particles (

Figure 6(c), L2), in a comparable result to that observed during LPD testing.

The sFDG profiles can be divided into three regions, as marked on the figures, in an analogous manner to the LPD profiles. These lab scale sFDG tests can consequently help to explain some of the behaviours observed during pilot-scale LPD measurements:

i.   Initially, the layer swells rapidly in response to its new environment. Significant removal, and hence changes in the phosphorescent intensity, must wait until the layer has swollen. There is a difference in timescales between the two techniques as NaOH displaces water in LPD tests, whereas in the sFDG experiments the layers are initially dry and are contacted with water or NaOH solution.

ii.   Both LPD and sFDG tests show a similar period of rapid layer removal, where the swollen, soft material can be readily removed by the flow of cleaning solution. Swelling does not need to be complete before removal starts.

iii. The final slow decay observed during both types of tests represents the removal of any residual material from the substrate.

A similar three-stage cleaning process has previously been reported during the alkaline cleaning of proteinaceous milk deposits by Xin *et al*. (2003) and Gillham *et al*. (1999).

A direct quantitative comparison between LPD and sFDG results is challenging, since the two techniques quantify cleaning progress using inherently different parameters. Identifying a cleaning time proved challenging for sFDG results, since the time taken to clean depends strongly on the local history of the layer, and in particular how frequently it has previously

been measured. The estimated soil removal rate, in μm/s, is a more suitable measure for this semi-quantitative comparison of the two techniques.

For sFDG testing, the removal rate (R_{FDG}) can be estimated directly from

Figure 6. For consistency, it is calculated based on the slope of the profile during a 30 s measurement period, once the layer thickness had reduced below 100 μm, and averaged over both replicates:

$$R_{FDG} = \left(\frac{d\delta}{dt} \right)_{\delta < 100 \mu m} \tag{2}$$

where δ is the layer thickness. While such a measure is subjective, and expected to exhibit a significant amount of scatter, it provides a simple, useful means of quantifying the differences between tests.

LPD quantifies the progress of cleaning via the decrease of layer phosphorescence. If the thickness of the swollen layer is estimated, based on sFDG measurements for the same material, then a physical removal rate during LPD testing can be inferred:

$$\left(\frac{d\delta}{dt} \right)_{LPD} = \delta_{max} \left(\frac{dI^*}{dt} \right)_{t=t_c}$$
$$= 0.368 \delta_{max} \left(\frac{r_c}{t_c} \right) \tag{3}$$

where δ_{max} is the maximum thickness of the layer in sFDG measurements (170 - 200 μm).

Such a method works well for the majority of LPD profiles, where the phosphorescence is described well by Equation (1). However, a more generally applicable method has been utilised in this work: namely, numerical calculation of the mean gradient of the LPD profile

14

(for all intervals with $dI^*/dt > $ s^{-1}). This method is used to obtain the characteristic removal rates (R_{LPD}) presented in Table 1 and Figure 7:

$$R_{LPD} = \delta_{max}\overline{\left(\frac{dI^*}{dt}\right)} \quad \forall\left(dI^*/dt\right) > 3s^{-1} \tag{4}$$

Figure 7 presents the removal rates estimated from LPD (open symbols, left y-axis) and sFDG (solid symbols, right y-axis) measurements. Different scales for each y-axis demonstrate the agreement between the two techniques. Both LPD and sFDG measurements indicate that samples containing small tracer particles (low S_a) tended to be removed more slowly than those containing large particles. This behaviour appears consistent, regardless of the type of tracer used, although there is significant scatter in the data. The graphical trend reflects observations made during both LPD and sFDG experiments, where layers containing large particulates were often cleaned significantly more easily than those containing small particles. These results suggest that the choice of tracer for LPD studies may influence cleaning by changing the soil's cohesive strength, or by altering the mechanical interaction between the soil and the cleaning solution.

3.3.   Comparison of LPD and FDG Testing

This study confirms LPD and sFDG to be complementary techniques. LPD provides information on the spatial distribution of soil coverage on a pilot scale, while sFDG allows more insight into the mechanism of soil removal. The measurement timescale for each technique is sufficiently fast for the experimental conditions employed in these tests: at higher cleaning rates (associated with larger cleaning fluid velocities and higher temperatures) each technique is likely to encounter a useful limit.

The liquid flow regimes in the two techniques differ considerably. LPD tests are performed under turbulent flow conditions ($Re \approx 26000$), while the flow through the nozzle throat during sFDG measurements is in the laminar regime ($Re \approx 500$). However, the shear stress exerted on the soil layer is comparable in both techniques, since the laminar flow in sFDG

measurements is confined to a narrow channel. The stress exerted during these sFDG measurements was estimated as 15 ± 5 Pa (Chew *et al.*, 2004), while that during LPD measurements can be estimated as 3.06 ± 0.02 Pa using the Colebrook-White equation for turbulent flow in pipes:

$$\tau_w = \tfrac{1}{4} f \tfrac{1}{2} \rho v^2 \tag{5a}$$

$$\frac{1}{\sqrt{f}} = -2\log\left(\frac{S_a}{3.7D_h} + \frac{2.51}{\mathrm{Re}\sqrt{f}}\right) \tag{5b}$$

where τ_w is the shear stress exerted by the fluid on the pipe wall, f is the Darcy friction factor, ρ and v are the liquid density and velocity respectively, D_h is the pipe hydraulic diameter, Re is the Reynolds number and the roughness height is represented by S_a.

These differences in shear stresses, and the associated differences in advection, are two factors that make direct quantitative comparison of the two techniques challenging. However, this work has illustrated the value of approaching an investigation using several complimentary techniques, where qualitative and quantitative information from sFDG tests has improved the understanding of pilot scale LPD studies.

4. CONCLUSIONS

This study has demonstrated the importance of a clear understanding of the nature of the soil removed during CIP, with particular emphasis in this work placed upon its roughness and composition. LPD and sFDG have been shown suitable for systematic comparisons of the ease of soil removal, and add to the scientific understanding of CIP.

Both LPD and sFDG tests demonstrated that starch layers containing large ZnS inclusions tended to be removed more readily than those containing smaller inclusions. FDG tests demonstrated the importance of the response of the soil to its environment, with layer swelling preceding the bulk of its removal. LPD tests identified a three-stage cleaning profile, which gave good agreement with a Weibull model of cleaning.

While the LPD and sFDG techniques consider different scales of cleaning, and employ different flow conditions in their study of CIP, this study illustrates the usefulness of such an interdisciplinary approach. sFDG tests aided the mechanistic understanding of LPD studies, while this pilot-scale work increased the applicability of the results to industrial CIP practice.

ACKNOWLEDGEMENTS

REFERENCES

Albert, F., Augustin, W., Scholl, S., 2011, Roughness and constriction effects on heat transfer in crystallization fouling, *Chemical Engineering Science*, 66, 499-509.

Bakker, D. P., van der Plaats, A., Verkerke, G. J., Busscher, H. J., van der Mei, H. C., 2003, Comparison of velocity profiles for different flow chamber designs used in studies of microbial adhesion to surfaces, *Applied Environmental Microbiology*, 69, 6280-6287.

Calvimontes, A., 2009, Topographic characterization of polymer materials at different length scales and the mechanistic understanding of wetting phenomena, PhD Thesis, Technische Universität Dresden, Section 2.4.3.

Chew, J. Y. M., Cardoso, S. S. S., Paterson, W. R., Wilson, D. I., 2004, CFD studies of dynamic gauging, *Chemical Engineering Science*, 59, 3381-3398.

Detry, J.G., Rouxhet, P.G., Boulangé-Petermann, L., Deroanne, C., Sindic, M., 2007, Cleanability assessment of model solid surfaces with a radial-flow cell, *Colloids and Surfaces A*, 302, 540-548.

Dürr, H., 2002, Milk heat exchanger cleaning: Modelling of deposit removal II, *Food and Bioproducts Processing*, 80, 253-259.

Fryer, P. J., Asteriadou, K., 2009, A prototype cleaning map: A classification of industrial cleaning processes, *Trends in Food Science and Technology*, 20, 255-262.

Gillham, C.R., Fryer, P.J., Hasting, A.P.M., Wilson, D.I., 1999, Cleaning-in-Place of whey protein fouling deposits: Mechanisms controlling cleaning, *Food and Bioproducts Processing*, 77 (2), 127-136.

Gordon, P.W., Brooker, A. D. M., Chew, Y. M. J., Wilson, D. I., York, D. W., 2010, A scanning fluid dynamic gauging technique for probing surface layers, *Measurement Science and Technology*, 21, 85-103.

Jurado, E., Bravo, V., Luzon, G., Fernández-Serrano, M., Garcia-Roman, M., Altmajer-Vaz, D., Vicaria, J. M., 2007, Hard-surface cleaning using lipases: enzyme-surfactant interactions and washing tests, *Journal of Surfactants and Detergents*, 10 (1), 61-70.

Liu, W., Christian, G. K., Zhang, Z., Fryer, P. J., 2006, Direct measurement of the force required to disrupt and remove fouling deposits of whey protein concentrate, *International Dairy Journal*, 16, 164-172.

Lohr, K. R., Rose, J. L., 2003, Ultrasonic guided wave and acoustic impact methods for pipe fouling detection, *Journal of Food Engineering*, 56, 315-324.

Mendret, J., Guigui, C., Schmitz, P., Cabassud, C., Duru, P., 2007, An optical method for in situ characterization of fouling during filtration, *AIChE Journal*, 53, 2265-2274.

Schöler, M., 2011. Analyse von Reinigungsvorgängen an komplexen Geometrien im immergierten System. Ph. D. thesis. Technische Universität Dresden.

Schöler, M., Föste, H., Manuel, M., Gottwald, A., Friedrichs, J., Werner, C., Augustin, W., Scholl, S., Majschak, J.-P., 2012, Local analysis of cleaning mechanisms in CIP processes, *Food and Bioproducts Processing*, 90 (4), 858-866.

Schöler, M., Fuchs, T., Helbig, M., Augustin, W., Scholl, S., Majschak, J.-P., 2009, Monitoring of the local cleaning efficiency of pulsed flow cleaning procedures, *Proc.* International Conference on Heat Exchanger Fouling & Cleaning 2009, Schladming, Austria.

Wilson, D. I., 2005, Challenges in cleaning: Recent developments and future prospects, *Heat Transfer Engineering*, 26, 51-59.

Xin, H., Chen, X. D., Özkan, N., 2003, A mathematical model of the removal of milk protein deposit, *Proc.* Heat Exchanger Fouling and Cleaning: Fundamentals and Applications, Santa Fe, USA.

FIGURES
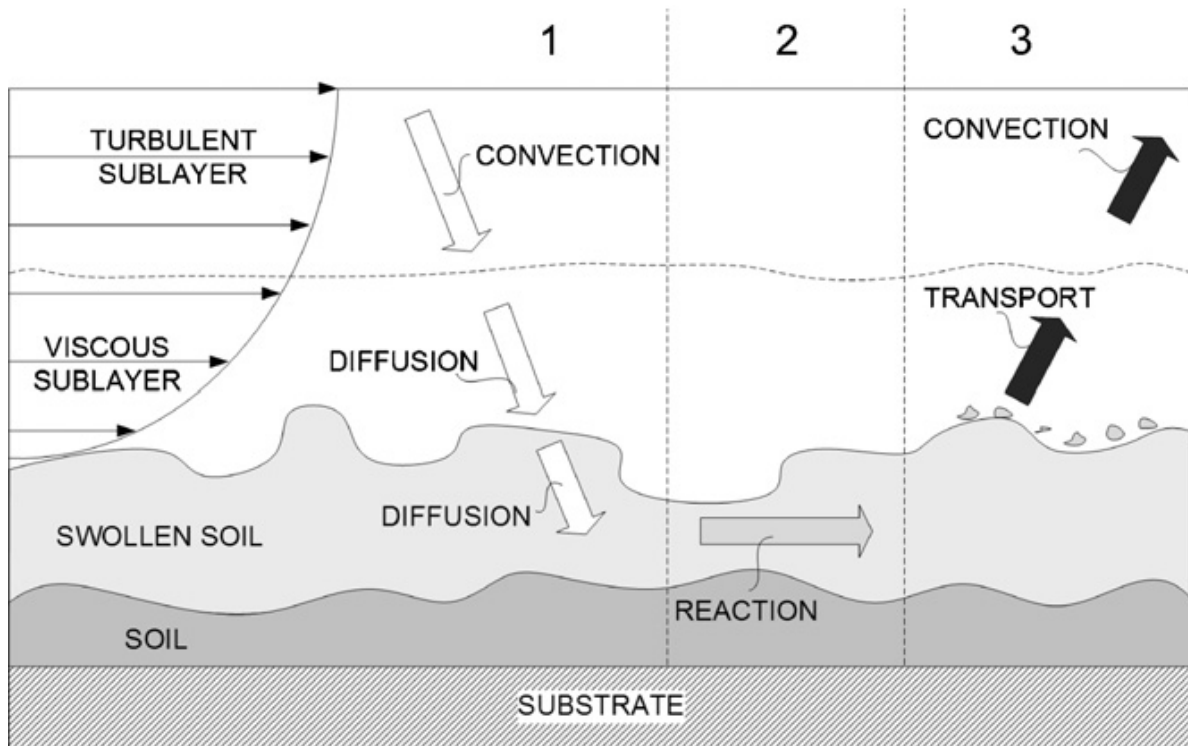
Figure 1: Mass transfer processes in the near-wall region during CIP (reproduced with permission from Schöler *et al*., 2012).
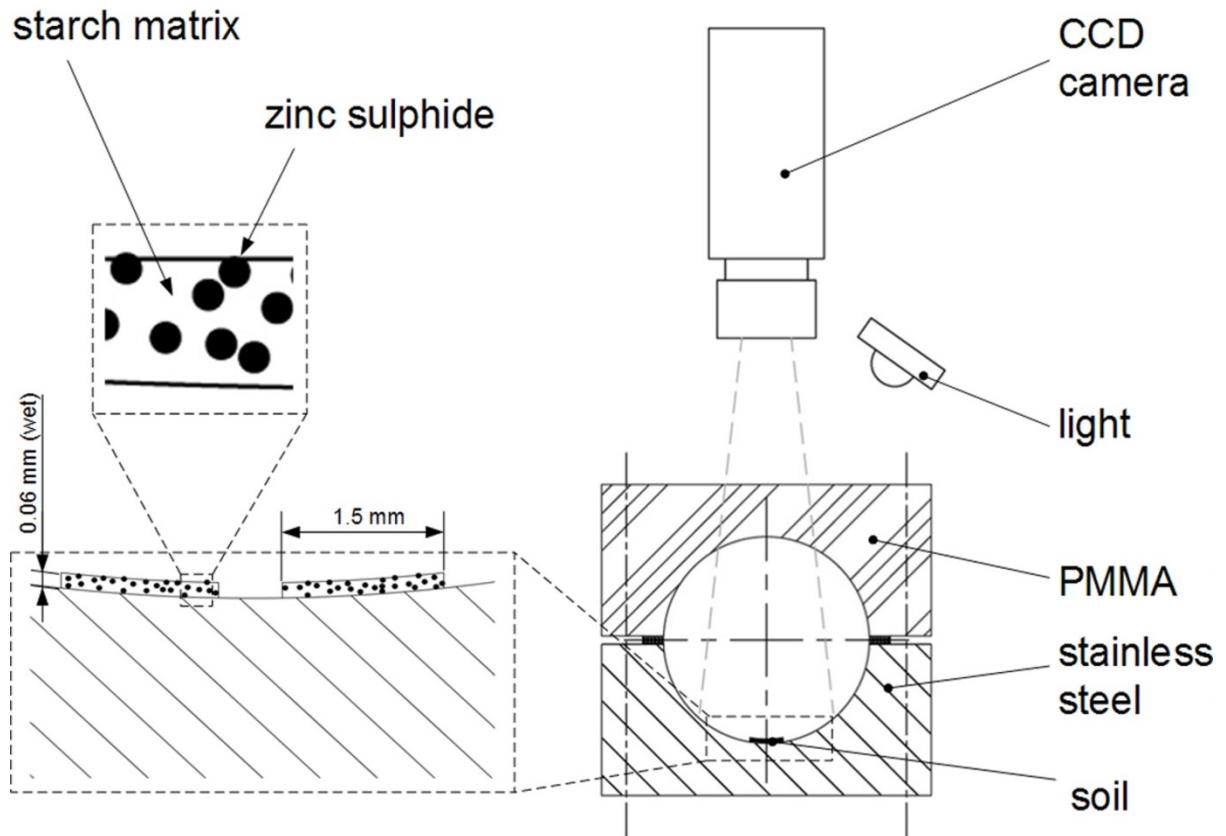
Figure 2: Cross-section of the LPD test section, showing the arrangement used for phosphorescence measurements (reproduced with permission from Schöler *et al.*, 2012).
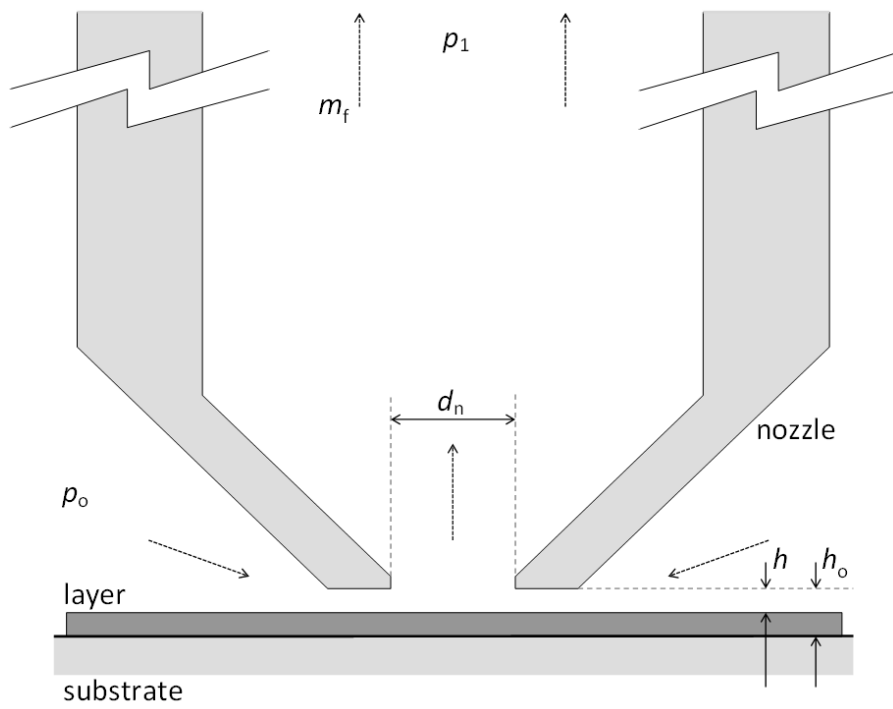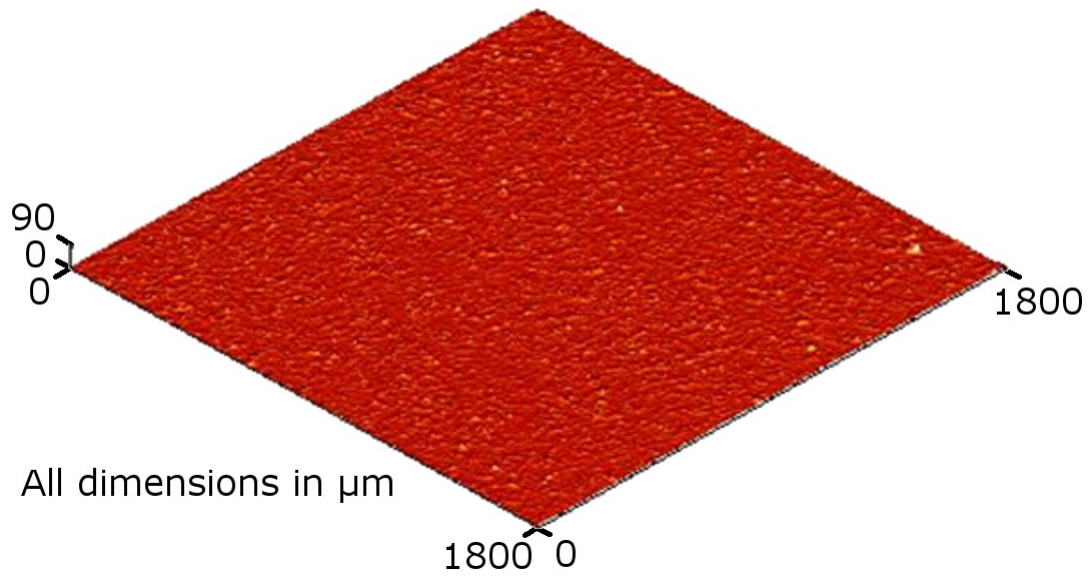
Figure 3: sFDG operating principles. A pressure gradient ($\Delta p_H = p_o - p_1$) draws cleaning fluid into the nozzle, at a rate governed by its proximity to the layer.
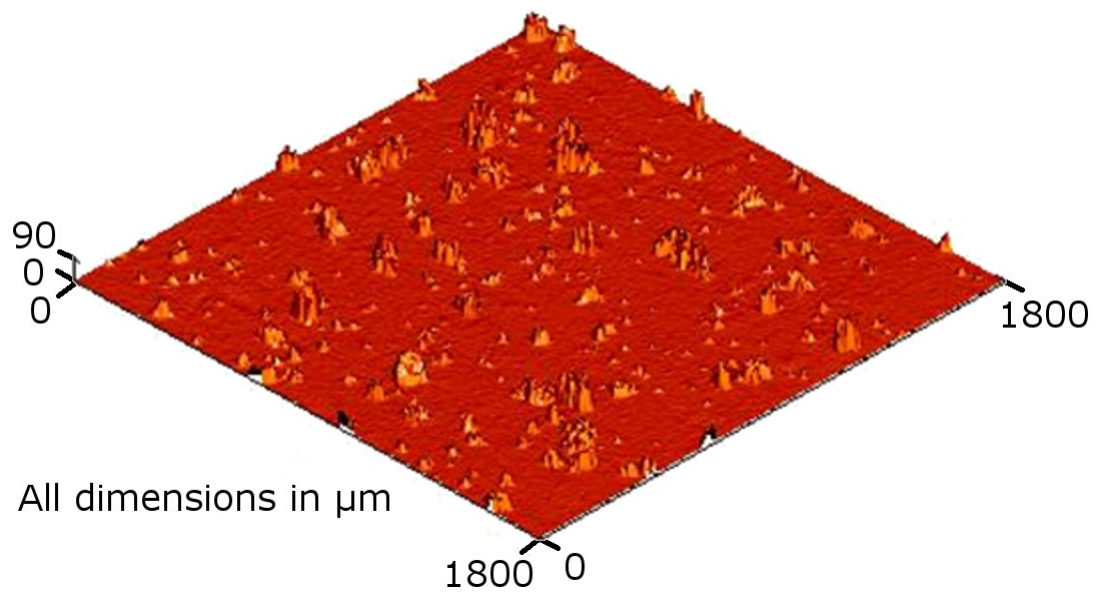
(a)

(b)

Figure 4: Chromatic white light sensor images of dry starch layers, containing (a) L2 (10 - 20 μm), and (b) L5 (50 - 80 μm) ZnS tracer particles.
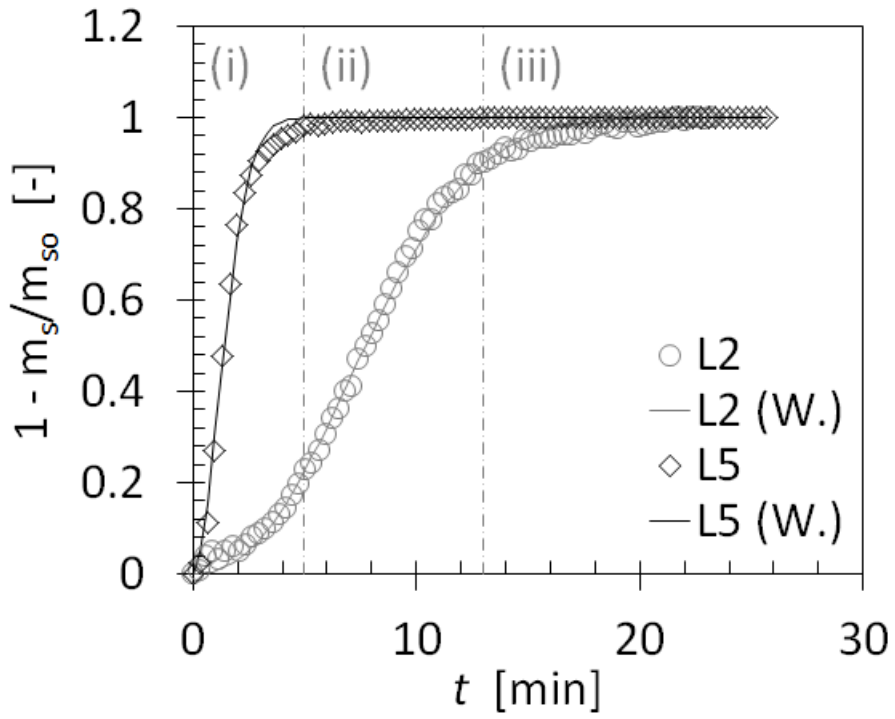
Figure 5: LPD measurements for the cleaning of the L2 and L5 layers. Solid lines indicate the Weibull models fitted to the data according to Equation (1), while vertical lines indicate (i) initial, (ii) removal, and (iii) decay phases for L2 only.
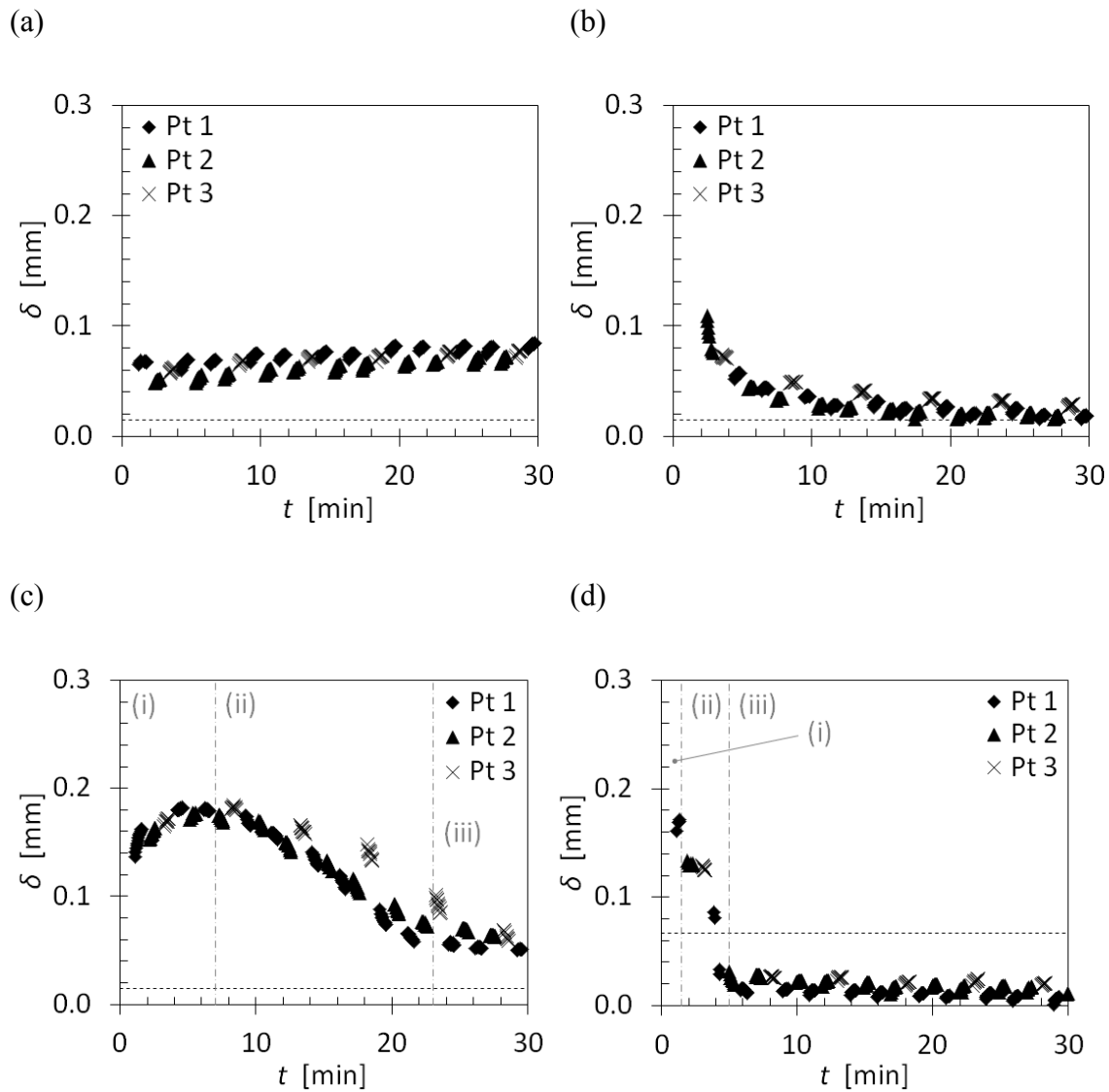
Figure 6: sFDG measurements of the thickness of starch-based layers during cleaning. (a) Rehydration of the starch layer in reverse osmosis water (pH 6.5). (b) A pure starch layer, without ZnS, in 0.5 wt% NaOH solution (pH 13.1). (c) Layer L2 in 0.5 wt% NaOH solution (pH 13.1). (d) Layer L5 in 0.5 wt% NaOH solution (pH 13.1). Solid symbols (Pt 1, Pt 2) show the thickness for points on the layer measured every cycle, while crosses (Pt 3) were measured once every two cycles. The dashed horizontal lines indicate the initial dry layer thickness, while vertical lines indicate (i) swelling, (ii) removal, and (iii) decay phases.
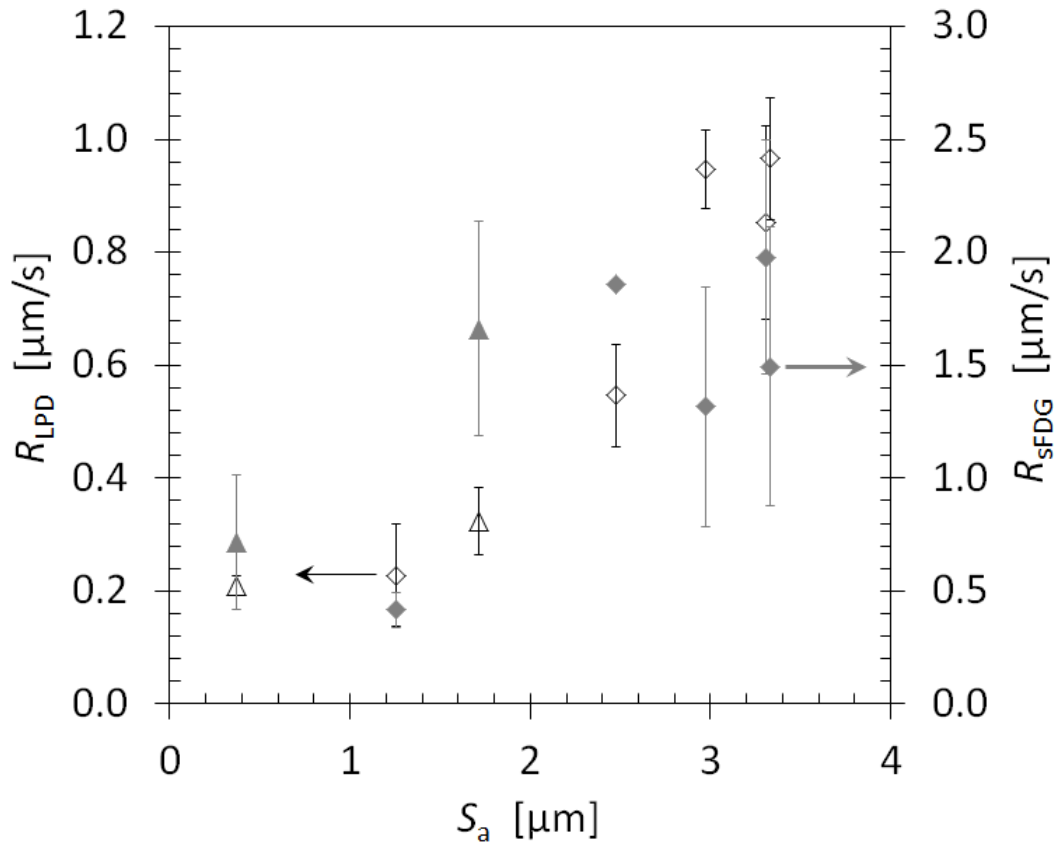
Figure 7: Effect of dry soil roughness on the removal rate during cleaning tests, as measured by LPD (left y-axis) and sFDG (right y-axis). Solid symbols indicate sFDG measurements, while open symbols denote LPD test results. Layers containing Lumilux and Storelite particles are distinguished by the use of diamond and triangular symbols respectively.

26

TABLES

Table 1: Summary and characterisation of the soil layers.

Ref.	Description	Particle Size Range[a]		Layer Roughness[b]		LPD Test Parameters				FDG Test Parameters	
		Min.	Max.	S_{pk}	S_a	τ_w	r_c	t_c	R_{LPD}	δ_{max}	R_{FDG}
		[μm]	[μm]	[μm]	[μm]	[Pa][c]	[-]	[s]	[μm s^{-1}]	[μm]	[μm s^{-1}]
L1	Lumilux N-FF	10	80	16.04	3.31	3.08	1.44	1.44	0.85	180	1.83
L2	Lumilux N-FF (sieved)	10	20	4.56	1.25	3.05	2.20	8.44	0.23	180	0.42
L3	Lumilux N-FF (sieved)	10	32	12.09	2.47	3.07	1.72	2.60	0.55	180	1.86
L4	Lumilux N-FF (sieved)	32	50	16.40	2.97	3.07	2.05	1.47	0.95	200	1.32
L5	Lumilux N-FF (sieved)	50	80	35.35	3.33	3.08	2.08	1.69	0.97	180	1.49
S6	Storelite HS-FF	1	10	1.19	0.37	3.04	2.02	8.90	0.21	180	0.71
S7	Storelite HS-F	20	40	7.69	1.71	3.06	1.92	5.09	0.32	170	1.66

[a] Determined by sieve analysis. [b] Measured for the dry layers by chromatic white light sensor (10 nm perpendicular resolution, 2 μm lateral resolution). [c] Estimated using Equation (4).